Structural study of $La_{0.75}Sr_{0.25}CrO_3$ at high temperatures

2006 J. Phys.: Condens. Matter 18 8661

(http://iopscience.iop.org/0953-8984/18/37/022)

INSTITUTE OF PHYSICS PUBLISHING JOURNAL OF PHYSICS: CONDENSED MATTER

J. Phys.: Condens. Matter **18** (2006) 8661–8672 doi:10.1088/0953-8984/18/37/022

Structural study of $La_{0.75}Sr_{0.25}CrO_3$ at high temperatures

Keka R Chakraborty[1], S M Yusuf[1], P S R Krishna[1], M Ramanadham[1], A K Tyagi[2,4] and V Pomjakushin[3]

[1] Solid State Physics Division, Bhabha Atomic Research Centre, Mumbai 400085, India
[2] Applied Chemistry Division, Bhabha Atomic Research Centre, Mumbai 400085, India
[3] Laboratory for Neutron Scattering, ETHZ&PSI, CH-5232 Villigen PSI, Switzerland

E-mail: aktyagi@barc.gov.in

Received 3 April 2006, in final form 26 July 2006
Published 1 September 2006
Online at stacks.iop.org/JPhysCM/18/8661

Abstract

A high-temperature neutron diffraction study has been carried out on $La_{0.75}Sr_{0.25}CrO_3$ compound in the temperature range 300–1400 K. On doping the parent compound $LaCrO_3$ with Sr at the La site, the orthorhombic (*Pbnm*) to rhombohedral ($R\bar{3}c$) structural transition shifts to lower temperatures. From quantitative Rietveld analysis it is found unequivocally that there is a two-phase coexistence (orthorhombic and rhombohedral phases with ∼89 and 11 weight%, respectively) in the temperature range 300–470 K and a three-phase coexistence (with a new cubic phase with space group *Pm3m*) in the temperature range 480–1400 K. The weight percentages of the orthorhombic, rhombohedral and cubic phases were found to be ∼49%, 37% and 14%, respectively, in the temperature range 480–1300 K, while over 1350–1400 K, the average weight percentages of orthorhombic, rhombohedral and cubic phases were found to be ∼41%, 41% and 18%, respectively. The coefficients of volume thermal expansion and linear thermal expansion have been determined for all three phases. The importance of the present study has been discussed for practical applications of the studied compound in solid oxide fuel cells.

(Some figures in this article are in colour only in the electronic version)

1. Introduction

$LaCrO_3$ is orthorhombic at room temperature, and undergoes crystallographic phase transitions first to the rhombohedral (hexagonal) phase at around 550 K and then to the cubic modification around 1300 K [1] (1873 K [2]). For $LaCrO_3$, the conductivity is not metallic although it has an incompletely filled d band. Goodenough [3, 4] showed that a combination of localized and collective (band) electronic models seemed to be appropriate to explain the conductivity behaviour for this compound.

[4] Author to whom any correspondence should be addressed.

Doping $LaCrO_3$ with Sr has been found to produce compounds with interesting physical properties, which are useful for various practical applications. The most effective dopant at the La^{3+}-site of $LaCrO_3$ is Sr^{2+}, which causes Cr ions to change from Cr^{3+} state to a mixed valence state of Cr^{3+} and Cr^{4+}. This produces enhanced p-type electrical conductivity. For example, $La_{0.84}Sr_{0.16}CrO_3$ was reported to have a high electronic conductivity at high temperatures and also exhibited excellent refractory properties [5]. This compound is, therefore, very useful as an electrode material for magnetohydrodynamic (MHD) power generation [6]. The other important aspects reported for this sample with respect to MHD electrodes are high density, adequate thermal shock resistance, chemical resistance to MHD gases, and decreased volatility. Sr-doped $LaCrO_3$ compounds have lately been mainly studied from the point of view of their use as interconnects in solid oxide fuel cells (SOFCs) operational at high temperatures [1, 7–9]. The compounds with relatively lower structural phase transition temperature would generate a stress and can affect the mechanical integrity of the high-temperature devices. Therefore, it is desired to tune the phase transition temperature in such compounds for their better operation in fuel cells. Structural study is, therefore, important to understand the details of the structural phase transitions in these suitably doped materials.

The ionic size of Sr^{2+} (1.44 Å) being larger than that of La^{3+} (1.36 Å), the tolerance factor t increases with increasing x. The tolerance factor t for the perovskite structure is defined as $t = (r_R + r_O)/\sqrt{2}(r_B + r_O)$, where r_R is the average ionic radius of the (La/Sr) site, r_O is the ionic radius of O^{2-}, and r_B is the average ionic radius of ions at the B (Cr)-site. The value of the tolerance factor for a cubic structure is $t = 1$. It is, therefore, possible to tune the structural phase transition temperatures in $La_{1-x}Sr_xCrO_3$ by a proper selection of the concentration of Sr. To the best of our knowledge there is no systematic structural study as a function of temperature on Sr-doped $LaCrO_3$ perovskites [10–14]. In the present paper, we report detailed structural study for the 25 mol% Sr^{2+} doped $LaCrO_3$ compound using high-temperature (300 K $\leqslant T \leqslant$ 1400 K) neutron diffraction. We present a quantitative analysis of the temperature dependence of various structural parameters along with the coefficients of linear thermal expansion along the unit cell directions and volume thermal expansion for all the phases. The usefulness of the observed results with regard to practical applications of the studied Sr-doped $LaCrO_3$ perovskite has been emphasized.

2. Experimental details

A polycrystalline sample of $La_{0.75}Sr_{0.25}CrO_3$ was synthesized by the solid state synthesis route. Moisture-free 99.9% pure powders of the reactants, namely, La_2O_3, $SrCO_3$ and Cr_2O_3, were taken in the appropriate stoichiometric proportions and ground in an agate mortar and pestle for one hour. They were then pelletized and heated for 48 h in a furnace at 1423 K in static air. Room-temperature x-ray diffraction patterns were recorded and the samples were found to be crystalline.

Neutron diffraction data were collected using a high-resolution HRPT diffractometer (high-resolution powder diffractometer using thermal neutrons) [15] at the SINQ spallation source at the Paul Scherrer Institut (Switzerland). The HRPT diffractometer was used in the high intensity mode ($\Delta d/d \geqslant 2 \times 10^{-3}$) with neutron wavelength $\lambda = 1.494$ Å. The powder sample was packed in vanadium cans and exposed to a neutron beam within a furnace. Diffraction measurements were carried at several temperatures over the range 300–1400 K in the heating cycle. Data at each temperature were collected for a fixed monitor. The data were reduced using standard procedures available on site to obtain intensity versus scattering angle 2θ in equal steps of 0.05°. Rietveld refinement of the neutron diffraction data was performed with the FULLPROF program [16] in the WINPLOTR suite of programs using the multiphase refinement mode.

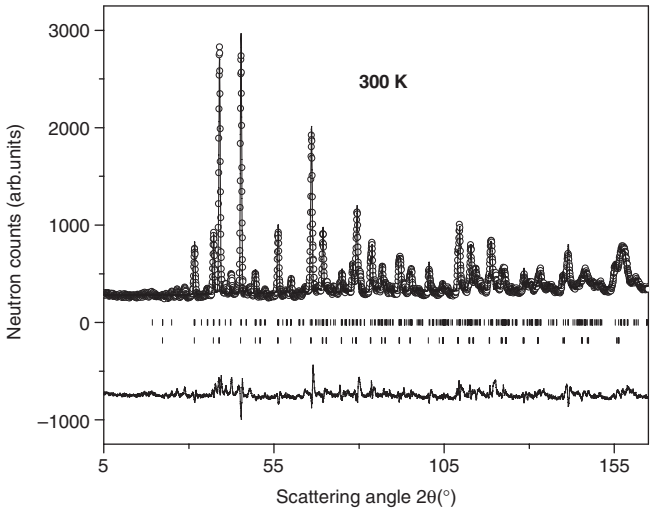

Figure 1. Neutron diffraction patterns at 300 K for the $La_{0.75}Sr_{0.25}CrO_3$ compound. The open circles are the observed data, and the continuous line is the Rietveld refined pattern. The difference pattern between the observed and calculated patterns is shown below. The difference pattern is shifted below for the sake of clarity. The two sets of vertical bars are the positions of the allowed Bragg peaks for the orthorhombic (top) and rhombohedral (bottom) phases.

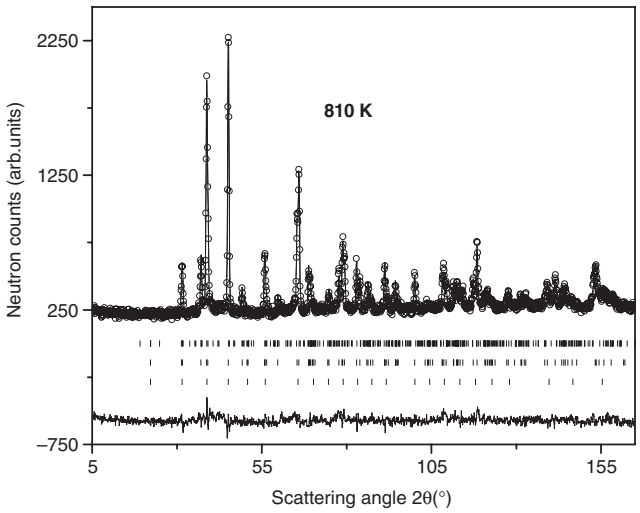

Figure 2. Observed (open circles) neutron diffraction pattern at 810 K. The continuous line is the Rietveld refined pattern. The difference pattern is shown below as a solid line. The difference pattern is shifted below for the sake of clarity. The vertical bars are the peak markers for the orthorhombic (top), rhombohedral (middle) and cubic (bottom) phases.

3. Results and discussion

Figure 1 shows the observed and Rietveld refined neutron diffraction patterns for the compound $La_{0.75}Sr_{0.25}CrO_3$ at room temperature. Rietveld refinement shows the presence of two crystallographic phases. The major phase was found to be the orthorhombic phase with a

Table 1. Structure parameters from Rietveld refinement at 300 K.

	Orthorhombic	Rhombohedral
Sp.Gr	*Pbnm*	$R\bar{3}c$
	La/Sr	
x	−0.0027(9)	0
y	0.0148(6)	0
z	0.25	0.25
B (Å)^2	0.6(1)	2.0(1)
	Cr	
x	0	0
y	0.5	0
z	0	0
B (Å^2)	0.92(2)	1.2(2)
	O1	
x	0.0599(8)	0.439(4)
y	0.500(1)	0
z	0.25	0.25
B (Å^2)	0.88(6)	2.9(1)
	O2	
x	0.2732(8)	
y	−0.2692(9)	
z	−0.0351(4)	
B (Å^2)	1.3 (6)	
a (Å)	5.5174(1)	5.506(1)
b (Å)	5.4795(1)	5.506(1)
c (Å)	7.7622(2)	13.515(4)
V (Å^3)	234.660(8)	354.8(1)
R_p	6.47%	
R_{wp}	8.54%	
R_e	5.01%	
χ^2	2.90	
R_{Bragg}	17.5%	12.9%
Wt%	89(1)%	11(1)%

weight percentage of 89(1)%. The minor phase was found to be rhombohedral with a weight percentage of ∼11(1)%. The structural parameters are listed in table 1. Neutron diffraction patterns for the sample at 810 K are shown in figure 2. Rietveld refinement shows the presence of three crystallographic phases (orthorhombic phase with 49(1) wt%, rhombohedral phase with 37(1) wt% and, cubic phase with 14(1) wt%). Table 2 lists the derived structural parameters for the sample at 810 K. Figure 3 depicts the neutron diffraction patterns at 1250 K, where the phase fractions for the above three phases were found to be same as at 810 K. However, there were variations in the other structural parameters. Table 3 tabulates all the derived structural parameters at this temperature (1250 K).

Figure 4 shows the evolution of weight percentages of the three phases as a function of temperature. Over 300–470 K, the weight percentages of the orthorhombic and rhombohedral phases were found to remain fixed at 89(1)% and 11(1)%, respectively. Around 470 K, the weight fraction of the orthorhombic phase was found to decrease with increasing temperature,

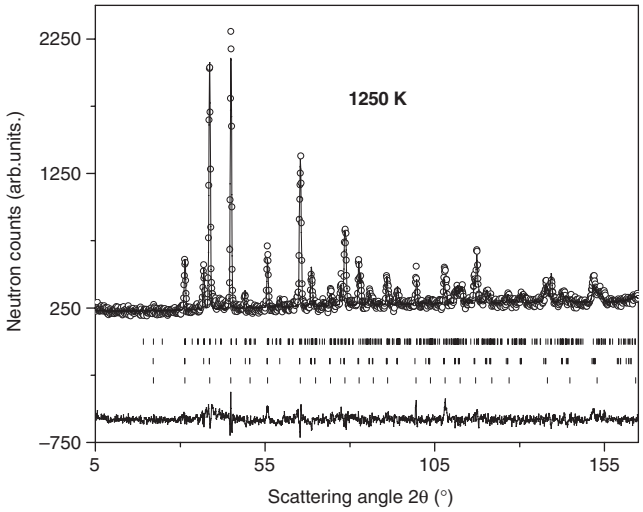

Figure 3. The open circles are the observed data at 1250 K, and the continuous line is the Rietveld refined pattern. The difference pattern is shown below by a solid line. The difference pattern is shifted below for the sake of clarity. The vertical bars are the Bragg peak positions for the orthorhombic (top) rhombohedral (middle) and cubic (bottom) phases.

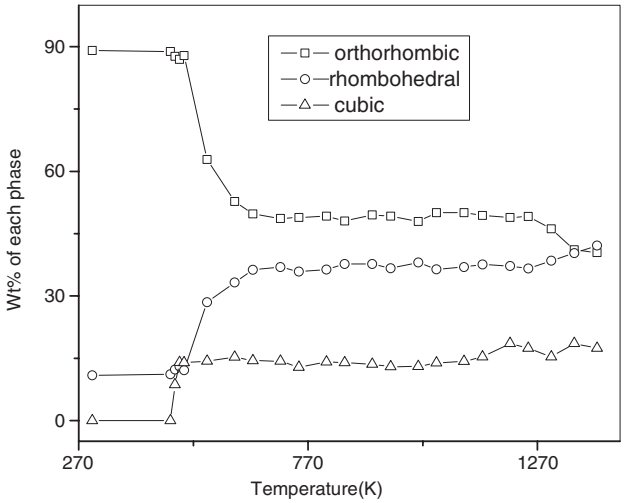

Figure 4. Weight fractions of the orthorhombic, rhombohedral and cubic phases as a function of temperature obtained from Rietveld refinement.

while the rhombohedral phase increased and a cubic phase appeared. Up to ∼1250 K, the cubic phase fraction was stable at 14(1) weight%. However, beyond 480 K (up to a temperature of ∼610 K) the phase fraction of the rhombohedral phase continued to increase to a value of ∼37 weight% while that of the orthorhombic phase decreased to a value of ∼49 weight%. It can be seen that in the temperature range 610–1250 K the weight fractions of all three phases are almost stable within the detection limit of the diffraction technique. Beyond 1300 K, the average weight percentages of the orthorhombic, rhombohedral and cubic phases were 41(1)% and 41(1)% and 18%, respectively.

Table 2. Structural parameters from Rietveld refinement at 810 K.

	Orthorhombic	Rhombohedral	Cubic
Sp.Gr	*Pbnm*	$R\bar{3}c$	*Pm3m*
		La/Sr	
x	−0.003(2)	0	0
y	−0.003(2)	0	0
z	0.25	0.25	0
B (Å^2)	0.9(2)	2.3(4)	1.1(4)
		Cr	
x	0	0	0.5
y	0.5	0	0.5
z	0	0	0.5
B (Å^2)	0.7(3)	0.4(4)	3.9(1)
		O1	
x	0.055(2)	0.432(1)	0.5
y	0.480(3)	0	0.5
z	0.25	0.25	0.25
B (Å^2)	0.8(1)	2.3(2)	3.2(4)
		O2	
x	0.255(6)		
y	−0.260(4)		
z	−0.023(1)		
B (Å^2)	2.0(2)		
a (Å)	5.5442(3)	5.5322(2)	3.9035(2)
b (Å)	5.4734(2)	5.5322(2)	3.9035(2)
c (Å)	7.7731(4)	13.577(1)	3.9035(2)
V (Å^3)	235.88(2)	359.86(4)	59.479(7)
R_p	8.13%		
R_{wp}	10. 4%		
R_e	5.66%		
χ^2	3.39		
R_{Bragg}	21.8%	17.9%	9.09%
Wt%	49(1)%	37(1)%	14(1)%

The unit cell parameter values, obtained from Rietveld refinement of the observed diffraction data over the entire temperature range of 300–1400 K, are depicted in figures 5, 6 and 7 for the orthorhombic, rhombohedral and cubic phases, respectively. The temperature variation of cell constants of the orthorhombic phase showed sudden changes between 480 and 610 K when a large part of the orthorhombic phase transforms to the rhombohedral phase. However, the cell constants and cell volumes of each phase increase linearly with increasing temperature at $T < 480$ K as well as at $T > 610$ K. For each phase, the coefficients of linear thermal expansion along respective crystallographic axes have been obtained by fitting the linear portion of cell constant versus temperature variation to a straight line. The coefficient of volume thermal expansion has similarly been obtained by fitting the observed linear portion of cell volume versus temperature curve to a straight line. In both cases, the fits are excellent for all three phases as shown in the lower panel of figure 5 for the orthorhombic phase, and in the insets of figures 6 and 7 for the rhombohedral and cubic phases, respectively.

Table 3. Structural parameters from Rietveld refinement at 1250 K.

	Orthorhombic	Rhombohedral	Cubic
Sp.Gr	*Pbnm*	$R\bar{3}c$	*Pm3m*
		La/Sr	
x	−0.002(3)	0	0
y	0.003(5)	0	0
z	0.25	0.25	0
B (Å^2)	1.1(2)	2.1(2)	2.6(9)
		Cr	
x	0	0	0.5
y	0.5	0	0.5
z	0	0	0.5
B (Å^2)	0.9(3)	1.5(4)	4(1)
		O1	
x	0.053(3)	0.441(1)	0.5
y	0.492(5)	0	0.5
z	0.25	0.25	0.25
B (Å^2)	1.3(2)	2.9(2)	3.3(7)
		O2	
x	0.265(3)		
y	−0.270(2)		
z	−0.018(2)		
B (Å^2)	2.0(2)		
a (Å)	5.5599(3)	5.5505(3)	3.9195(2)
b (Å)	5.5139(2)	5.5505(3)	3.9195(2)
c (Å)	7.8191(4)	13.627(1)	3.9195(2)
V (Å^3)	239.70(2)	363.58(4)	60.21(1)
R_p	6.06%		
R_{wp}	7.75%		
R_e	5.64%		
χ^2	1.89		
R_{Bragg}	15.7%	12.8%	7.09%
Wt%	49(2)%	37(2)%	14(2)%

The lattice constant b of the orthorhombic phase expands by 1.03% in the temperature range 610–1250 K. It expands most in comparison with a and c in the orthorhombic phase as well as any of the cell constants of the other two phases in the temperature range 610–1250 K. This reflects the fact that as temperature is raised there is no isotropic expansion of the unit cell. In the same temperature range, 610–1250 K, the orthorhombic unit cell volume also expands (1.86%) more than the rhombohedral phase (1.47%). When compared with the cubic phase, however, among the three phases, the volume expansion is highest in the cubic phase (∼2.17%).

For the orthorhombic phase, the tilt angles of the CrO_6 octahedra in the perovskite structure as a function of temperature have been derived, and they are plotted in figure 8. The tilt angles are defined as $[180 - (\text{Cr–O1–Cr})]/2$ and $[180 - (\text{Cr–O2–Cr})]/2$ degrees, where (Cr–O1–Cr) and (Cr–O2–Cr) are the axial and in-plane (a–b plane) bond angles, respectively, between Cr, O and Cr ions in the perovskite structure. Figure 9 shows the part of the unit cell showing the Cr–

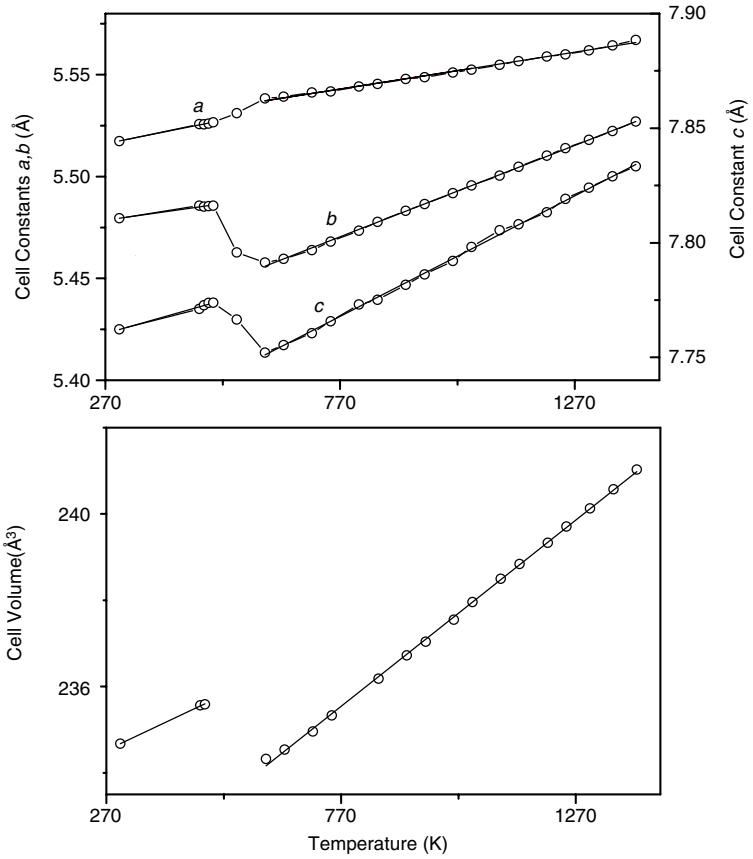

Figure 5. Unit cell constants of the orthorhombic phase of $La_{0.75}Sr_{0.25}CrO_3$ as a function of temperature. The observed data fit to a straight line below 480 K and from 610 K onwards. The lower panel shows the cell volume V as a function of temperature with a linear fit to data in both temperature ranges, namely below 480 K and above 610 K.

O1–Cr and Cr–O2–Cr bond angles. Figure 8 shows an abrupt drop in tilt angle Cr–O_2–Cr around 490 K where a large fraction of the sample transforms to a rhombohedral phase, whereas, no such drastic variation has been found for the tilt angle Cr–O_1–Cr. The Cr–O_1 bond length shows a negligible variation as a function of temperature, whereas one of the Cr–O_2 bond lengths shows an abrupt rise around 490 K and then a fall with increase in temperature while the other Cr–O_2 bond shows an abrupt fall at 490 K with a rise after that, also corroborating the temperature dependence of the Cr–O2–Cr tilt angle. The three Cr–O bond lengths (one axial and two in the basal plane) for the orthorhombic phase have been plotted as a function of temperature in figure 10. The contrasting changes with temperature of the two tilt angles, Cr–O1–Cr and Cr–O2–Cr, indicate a buckling of the CrO_6 octahedra only in the basal (a–b) plane. Table 4 lists the derived thermal expansion coefficients. This coefficient is defined as follows:

$$\alpha = (a_T - a'_T)/(T - T')a_T \tag{1}$$

where a_T is the cell constant at temperature T and a'_T is the cell constant at temperature T'. In the case of volume thermal expansion coefficient, a_T and a'_T are to be replaced by the unit cell volume V_T and V'_T, respectively. It is interesting to note that the linear expansion

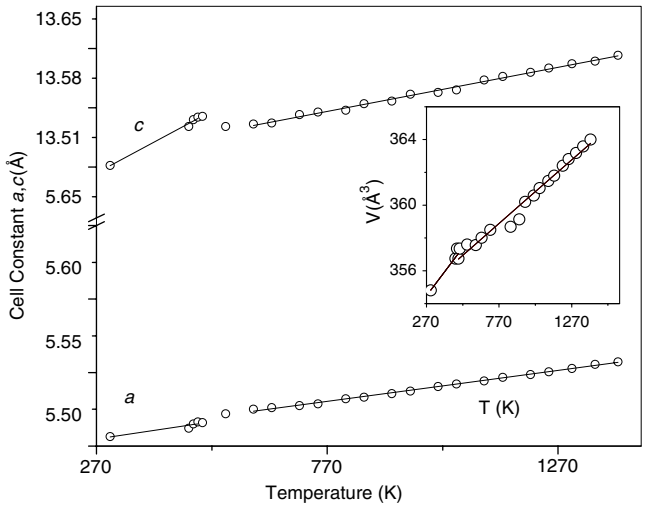

Figure 6. Unit cell constants of the rhombohedral phase of $La_{0.75}Sr_{0.25}CrO_3$ as a function of temperature. The straight line is a fit to data. The temperature dependence of the cell volume V is shown in the inset with a linear fit to data.

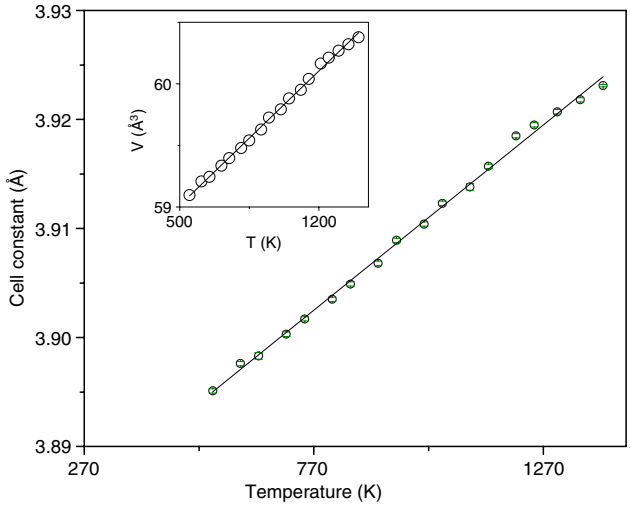

Figure 7. Unit cell constants of the cubic phase of $La_{0.75}Sr_{0.25}CrO_3$ as a function of temperature. The solid line is a linear fit to the observed data. The inset shows the temperature dependence of the unit cell volume V along with a straight line fit.

coefficient along the a axis is nearly same for the orthorhombic and rhombohedral phases in the temperature range 300–480 K. Similar behaviour has been found for all three phases over the higher temperature range of 610–1400 K.

The present investigation results in a deep insight into the intrinsic thermal expansion of $La_{0.75}Sr_{0.25}CrO_3$. It may be noted that one gets only a bulk thermal expansion behaviour from a dilatometric measurements [17, 10]. In order to prepare materials with tailored thermal expansion behaviour, it is required to study the intrinsic thermal expansion behaviour. In this regard the role of structure in governing the expansion behaviour needs to be probed, as done

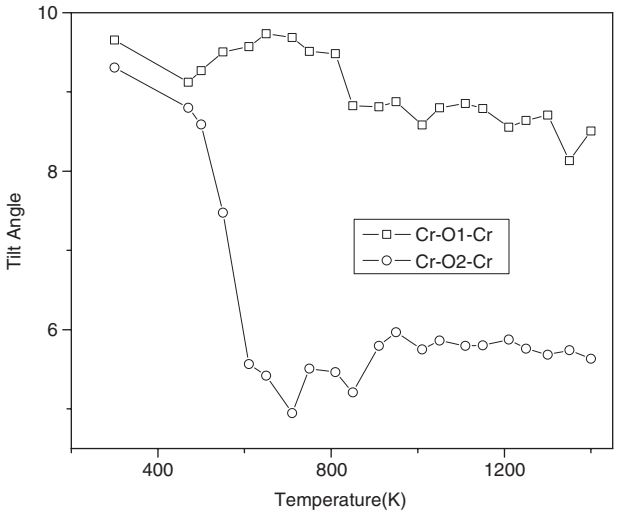

Figure 8. Tilt angles as a function of temperature.

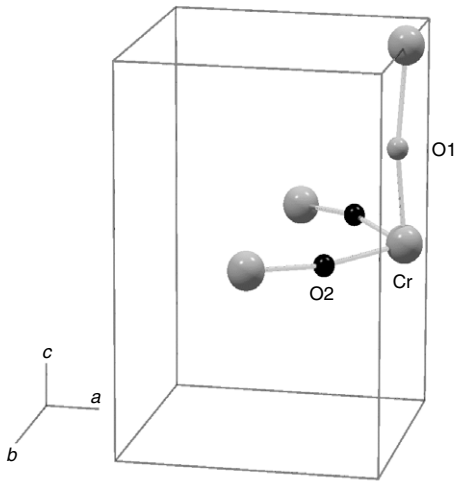

Figure 9. Cr–O bond lengths and Cr–(O1, O2)–Cr bond angles in the orthorhombic phase.

in the present work. For the present system we find that there is a reasonably good match of the linear and volume thermal expansion coefficients between the orthorhombic and rhombohedral phases over the entire temperature range. In solid oxide fuel cell (SOFC) devices, the thermal expansion coefficient of one crystallographic phase component must match that of the other phase. Otherwise, during an operation of these cells at high temperatures, different thermal expansion rates of different phase components would destroy the mechanical integrity of the cell. This information of an understanding of coefficients of thermal expansion over a wide range of temperature is useful for designing solid oxide fuel cells.

It was also observed that the relative weight percentages of all the three phases remain constant over 480 to 1300 K. The SOFC's operating temperature is about 1073 to 1173 K. Therefore, over this operating temperature range there is no change in weight fraction of

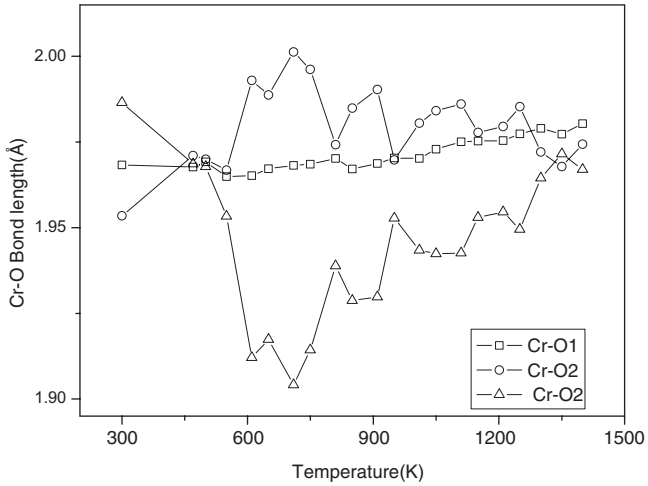

Figure 10. Cr–O bond lengths as a function of temperature.

Table 4. Thermal expansion coefficients of the three phases along the a, b and c crystallographic axes and volume thermal expansion coefficient.

Thermal expansion coefficients (K)	Orthorhombic phase RT–500 K	Rhombohedral phase RT–500 K	Orthorhombic phase 610–1400 K	Rhombohedral phase 610–1400 K	Cubic phase 550–1400 K
α_a	9.1×10^{-6}	9.1×10^{-6}	7.25×10^{-6}	7.26×10^{-6}	7.7×10^{-6}
α_b	5.5×10^{-6}		7.3×10^{-6}		
α_c	7.7×10^{-6}	21.5×10^{-6}	14.2×10^{-6}	7.4×10^{-6}	
α_V	21.9×10^{-6}	33.2×10^{-6}	36.9×10^{-6}	21.7×10^{-6}	26.7×10^{-6}

orthorhombic, rhombohedral and cubic phases. We strongly believe the results of the systematic phase evolution in $La_{0.75}Sr_{0.25}CrO_3$ as a function of temperature will also be useful in various applications, in particular SOFCs. Based on these results, one can design new substituents in order to stabilize a particular modification of $LaCrO_3$, depending on the requirement.

The electrical conductivity σ for $La_{1-x}Sr_xCrO_3$ compounds is found to vary smoothly $[\ln(\sigma T) \propto 1/T]$ in the entire high-temperature region covering the operating temperature for these compounds in SOFC devices [18, 19]. Similarly, a magnetic susceptibility study showed that these compounds undergo magnetic ordering only below room temperature [13], and the susceptibility obeys the Curie–Weiss law at higher temperatures [5]. It is, therefore, evident that the studied compound is free from any anomalies of magnetic and/or transport properties over the operating temperature range of the studied material, which makes it suitable in SOFC devices.

4. Summary and conclusions

A 25 mol% Sr doped $LaCrO_3$ sample has been synthesized and studied using high-resolution neutron diffraction over the temperature range 300–1400 K. The structural parameters for the orthorhombic, rhombohedral and cubic phases have been derived from Rietveld analysis. The cell constants have been found to show an abrupt change at 480 K in the orthorhombic

phase, signalling the onset of a cubic transition and enhancement of the rhombohedral phase. The linear and volume thermal coefficients have been measured; the data are very useful for designing solid oxide fuel cells using the studied material.

We have found from our quantitative data analysis that the compound does not show any change in the weight fractions of the three phases in the temperature range 610–1250 K, which covers the operating temperature range of this SOFC material. We have also found a reasonable match in the thermal expansion coefficients in the operating temperature range. There is no change in the magnetic phase in the operating temperature range. Also, there is no anomaly in the electrical conductance in the operating temperature of SOFCs for the studied compound. Therefore, this material is suitable for SOFC interconnects.

Acknowledgment

This work is based on experiments performed at the Swiss spallation neutron source SINQ, Paul Scherrer Institute, Villigen, Switzerland.

References

[1] Oikawa K, Kamiyama T, Hashimoto T, Shimojyo Y and Morii Y 2000 *J. Solid State Chem.* **154** 524
[2] Momin A C, Mirza E B and Mathews M D 1991 *J. Mater. Sci. Lett.* **10** 1246
[3] Goodenough J B 1966 *J. Appl. Phys.* **37** 1415
[4] Goodenough J B 1967 *Czech J. Phys.* B **17** 304
[5] Karim D P and Aldred A T 1979 *Phys. Rev.* B **20** 2255
[6] Meadowcroft D B 1969 *Brit. J. Appl. Phys., J. Phys. D* 2 **2** 1225
[7] Baker R T and Metcalfe I S 1995 *Appl. Catal.* A **126** 297
[8] Vernoux P, Guindet J and Kleitz M 1998 *J. Electrochem. Soc.* **145** 3487
[9] Primdahl S, Hansen J R, Grahl-Madsen L and Larsen P H 2001 *J. Electrochem. Soc.* **148** A74
[10] Mathews M D, Ambekar B R and Tyagi A K 2002 *Thermochim. Acta* **390** 61
[11] Khattak C P and Cox D E 1977 *Mater. Res. Bull.* **12** 463
[12] Khattak C P and Cox D E 1977 *J. Appl. Crystallogr.* **10** 405–11
[13] Tezuka K, Hinatsu Y, Nakamura A, Inami T, Shimojo Y and Morii Y 1998 *J. Solid State Chem.* **141** 404–10
[14] Maiti K and Sarma D D 1996 *Phys. Rev.* B **54** 7816
[15] Fischer P, Frey G, Koch M, Konnecke M, Pomjakushin V, Schefer J, Thut R, Schulmpf N, Buerge R, Grueter U, Bondt S and Berruyer E 2000 *Physica* B **276–278** 146
[16] Roisnel T and Rodriguez-Carvajal J 2001 *J. Mater. Sci. Forum* **378–381** 118
[17] Hayashi H, Watanabe M, Ohuchida M, Inaba H, Hiei Y, Yamamoto T and Mori M 2001 *Solid State Ion.* **144** 301
[18] Bansal K P, Kumari S, Das B K and Jain G C 1983 *J. Mater. Sci.* **18** 2095
[19] Liu X, Su W, Lu Z, Liu J, Pei L, Liu W and He L 2000 *J. Alloys Compounds* **305** 21